

Quantum Dynamics of Disordered Bosons in an Optical Lattice

Chien-Hung Lin^{1,2}, Rajdeep Sensarma¹, K. Sengupta³ and S. Das Sarma^{1,2}

1. Condensed Matter Theory Center, Department of Physics, University of Maryland, College Park, USA 20742
2. Joint Quantum Institute, University of Maryland, College Park, USA 20742
3. Theoretical Physics Department, Indian Association for the Cultivation of Science, Kolkata 700032, India

(Dated: November 5, 2018)

We study the equilibrium and non-equilibrium properties of strongly interacting bosons on a lattice in presence of a random bounded disorder potential. Using a Gutzwiller projected variational technique, we study the equilibrium phase diagram of the disordered Bose Hubbard model and obtain the Mott insulator, Bose glass and superfluid phases. We also study the non equilibrium response of the system under a periodic temporal drive where, starting from the superfluid phase, the hopping parameter is ramped down linearly in time, and back to its initial value. We study the density of excitations created, the change in the superfluid order parameter and the energy pumped into the system in this process as a function of the inverse ramp rate τ . For the clean case the density of excitations goes to a constant, while the order parameter and energy relaxes as $1/\tau$ and $1/\tau^2$ respectively. With disorder, the excitation density decays exponentially with τ , with the decay rate increasing with the disorder, to an asymptotic value independent of the disorder. The energy and change in order parameter also decrease as τ is increased.

PACS numbers:

I. INTRODUCTION

The model of bosons on a lattice interacting repulsively through a local interaction in the background of a random one-body disorder potential (or the disordered Bose Hubbard model [1]) has been used as a paradigm for superfluid insulator transition in a host of disordered quantum systems. These encompass a number of different condensed matter systems, from ^4He on disordered substrates [2] or in porous media [3], to dirty superconducting films [4] and Josephson junction arrays [5], to disordered quantum magnets [6]. In fact, this model has often been used to describe the relevant bosonic degrees of freedom near phase transitions in strongly disordered systems. There are three main ingredients in this model: a hopping or kinetic energy term for bosons, which tend to favour delocalized superfluid phases, an onsite repulsion which tries to localize the bosons to create a Mott insulator, and an onsite one-body random disorder potential which scatters the bosons and lead to loss of coherence of the superfluid. The interplay of these three different terms produces a rich phenomenology in these systems, both in its equilibrium properties and in terms of non equilibrium dynamics in these systems.

Beyond the traditionally material based phenomena, for which it serves as a paradigm, the disordered Bose Hubbard model can be realized with ultracold atomic systems [7–9], which have emerged as the new platform to study the behaviour of model many-body Hamiltonians used in condensed matter physics and elsewhere [10]. The easy tunability of implemented Hamiltonian parameters and almost complete isolation from external environment makes these systems attractive candidates to simulate strongly interacting quantum many body Hamiltonians, both on the lattice and in the continuum. Although cold-atomic systems on optical lattices are generally free of disorder (which is inevitably present in solid state systems), disorder can be added in a controlled manner either by use of speckle potentials [8, 9] or by the use of multiple op-

tical lattice beams with incommensurate wavelengths [7, 11]. In either case, the disorder potential (or its distribution in the case of speckle potentials) is well characterized and the parameters characterizing the disorder potential can be changed in a controlled way, in contrast to condensed matter systems, where the disorder parameters are unknown a-priori, and are mostly determined through a post-hoc process of matching experimentally measured quantities (like transport co-efficients) to theoretical model calculations. The possibility of controlled addition of disorder, thus, makes cold atoms uniquely suited to study the effects of disorder on strongly interacting quantum many-body systems.

Cold atom systems also provide an added advantage of easy access to the internal nonequilibrium dynamics of isolated interacting systems. The low energy scales (in the absolute sense), the easy tunability of the Hamiltonian parameters and the almost complete isolation of the system from external environment make it very easy to perturb the system from its equilibrium state in a well characterized way and then follow the dynamics of the system without the help of ultrafast probes. This has opened up the possibility of studying the quantum dynamics of these systems out of equilibrium [12, 13].

Since the early work of Fisher *et al* [1], the equilibrium properties of the disordered Bose Hubbard model has been treated with various levels of sophistication from mean field theory [14–16] to strong coupling expansions [17] to Monte Carlo techniques [18–20]. In this paper, we provide an alternative approach to studying the disordered Bose Hubbard model based on variational wavefunctions. Our approach is applicable in the strongly interacting limit of the model, but does not place any constraint on the strength of disorder potential. The variational approach uses a canonical transformation to systematically eliminate processes connecting states with large energy difference ($\sim U$, the onsite Hubbard repulsion, or more) and generates an effective low energy Hamiltonian for the system in the strongly interacting limit. This effective Hamiltonian is then treated with a Gutzwiller mean

field wavefunction. There are several benefits to this approach over other standard approaches : i) It captures the strong correlations generated by the boson repulsion more accurately than mean field theory ii) The requirement of disorder average makes the problem numerically very resource intensive to treat beyond mean field theory. Our semi-analytic approach lessens the numerical burden, while keeping essential “beyond mean field” correlations. iii) Since this approach generates an effective low energy Hamiltonian, it can be easily modified to study quantum dynamics in these systems. This is a crucial aspect of this approach, which makes it qualitatively different from more sophisticated Monte Carlo techniques, specially in larger than one dimensions.

In this paper, we first study the equilibrium phase diagram of the 2D disordered Bose Hubbard model on a square lattice within our approach as a function of U/J and the chemical potential μ for different values of the disorder strength V . This yields three phases: (a) an incompressible phase incoherent Mott insulating phase at large interaction strength, whose area decreases with increasing disorder strength (b) a superfluid phase, with coherent condensation of the bosons into a single quantum state at small interaction strength, and (c) a Bose glass phase in between them, where the system is compressible, but the phase coherence of the bosonic condensate is completely destroyed. We also study the non-equilibrium dynamics of the system under the following conditions: the system is initialized in its ground state in the superfluid phase. The interaction parameter is ramped up linearly in time to a very high value and then ramped back linearly to its initial value. At the end of this process, we study the density of excitations produced in the system, the energy pumped into the system and the deviation of the superfluid order parameter from its initial value, as a function of the rate of the ramp, $1/\tau$. In the clean case, the excitation density goes to a constant, while the order parameter deviation and energy scales as $1/\tau$ and $1/\tau^2$ in the large τ limit. With disorder, the excitation density shows an exponential decay. The energy and order parameter deviation also decreases with increasing τ , although a scaling form is hard to obtain due to inherent noise in the data.

The paper is organized as follows: In section II, we present our variational wavefunction approach and introduce the canonical transformation. Section III presents the details of obtaining the canonical transformation operator and the effective low energy Hamiltonian. In section IV, we present the equilibrium phase diagram calculated within our approach. In section V we present the results for the non equilibrium dynamics in the system. Finally, we conclude in section VI with a summary of our results and a discussion of limitations of the present formalism and ways to improve it.

II. VARIATIONAL WAVEFUNCTION

The Hamiltonian of the disordered Bose Hubbard model on a square lattice is given by

$$H = -J \sum_{\langle ij \rangle} b_i^\dagger b_j + \frac{U}{2} \sum_i \hat{n}_i (\hat{n}_i - 1) + \sum_i (v_i - \mu) \hat{n}_i \quad (1)$$

where b_i^\dagger creates a boson on site i and \hat{n} is the boson number operator. Here J is the nearest neighbour hopping energy scale, U the on-site Hubbard repulsion, μ the chemical potential and v_i is the random local potential on site i . v_i is a spatially uncorrelated random variable drawn from a uniform distribution in the range $-V/2 < v_i < V/2$, where V sets the energy scale for disorder effects.

The clean Bose Hubbard model ($v_i = 0$) has a quantum phase transition between a strongly interacting incompressible Mott insulating phase with commensurate integer filling at small J/U and a phase coherent superfluid state with large number fluctuations at large J/U . The transition is characterized by the vanishing of both the superfluid stiffness and the compressibility as one reaches the Mott phase. In the presence of disorder, there is an intervening Bose glass phase where the superfluid stiffness vanishes, but the compressibility remains finite.

We wish to study the equilibrium phases and dynamics in the disordered Bose Hubbard model through a variational wavefunction approach. For the equilibrium phase diagram at $T = 0$, we use a variational ground state wavefunction of the form

$$|\psi\rangle = e^{-iS} |\psi_0\rangle \quad |\psi_0\rangle = \prod_i \sum_n f_{ni} |n\rangle_i \quad (2)$$

Here $|\psi_0\rangle$ is a Gutzwiller type local mean field state with variational parameters f_{ni} , which satisfies $\sum_n |f_{ni}|^2 = 1$ to ensure normalization of the state, $|n\rangle_i$ is the number state with n bosons on site i , and e^{-iS} is a canonical transformation that builds in non-local correlations in the proximity of a Mott insulator.

The canonical transformation approach has a long history of use in the context of Fermi Hubbard model in the strongly interacting limit, where it is used to convert the Hubbard model to the so called “t-J” model used in the study of high temperature superconductors [21]. Recently this approach has been adapted successfully to study the equilibrium phases of and quantum dynamics in clean Bose Hubbard model [22, 23]. The canonical transform uses the local number states (which are eigenstates of the local part of the Hamiltonian) as the starting point. Note that in the present formulation of the canonical transformation, we do not use a particular local state as our starting point (except assuming a local number state), as is done in Ref. 22, where the atomic limit Mott phase ground state with the same number of particles on each site is used as the starting point. The hopping terms then start to build in correlations between different number states on neighbouring sites.

The hopping term can connect local number states which

differ in energy by $\sim U$ or higher. To see this consider a state with n_1 particles on site i and n_2 particles on site j and a hopping process where a particle hops from j to i . The energy difference (coming from the local part of the Hamiltonian) between the initial and final state is $\delta\epsilon = U(n_1 - n_2 + 1) + v_i - v_j$ and $|\delta\epsilon|$ can be $\sim U$ or more depending on n_1 and n_2 . We would like to note that, since we are interested in energy difference of states connected by hopping (which does not change the total number of particles in the system), the chemical potential drops out of the expression for the canonical transform. Hence our formalism is applicable for any μ , even to the parameter regime where $\mu \sim nU$, n being an integer.

The basic idea of the canonical transform is to eliminate terms in the Hamiltonian which connects local number states differing by a large energy ($\sim U$ or more) order by order in J/U through the canonical transformation. The easiest way to see this is to note that for any operator A ,

$$\langle\psi|A|\psi\rangle = \langle\psi_0|A^*|\psi_0\rangle, \quad \text{where } A^* = e^{i\mathcal{S}}Ae^{-i\mathcal{S}} \quad (3)$$

is the canonically transformed operator. For the Hamiltonian, H , the requirement that H^* does not have any terms connecting states which differ in energy by $\sim U$ fixes the form for \mathcal{S} . The low energy effective Hamiltonian, H^* , obtained by the canonical transform, not only allows the low energy hopping processes, but also builds in correlations from virtual transitions to high energy states. In the next section, we provide the details of the canonical transformation and the effective Hamiltonian for the disordered Bose Hubbard model. We would like to note here that although we will focus here on a random disorder potential, our formalism is capable of handling *any* one-body potential, e.g. it can be used to treat effects of harmonic traps in ultracold atomic gases in optical lattice.

III. THE CANONICAL TRANSFORMATION

The disordered Hubbard model can be separated into a local part containing the interaction and the one body potential and a kinetic energy part.

$$H = H_0 + \sum_{\langle ij \rangle} T_{ij}, \quad H_0 = \frac{U}{2} \sum_i \hat{n}_i(\hat{n}_i - 1) - \mu_i \hat{n}_i \quad (4)$$

where $\mu_i = \mu - v_i$, μ being the chemical potential and v_i the random disorder potential. It is also easy to see that the hopping term $T_{ij} = -Jb_i^\dagger b_j$ connects local states differing in energy by $\epsilon_{ij}^\alpha = \alpha U + v_i - v_j$, where $\alpha = 0, \pm 1, \pm 2, \dots$. This suggests breaking up the hopping term, $T_{ij} = \sum_\alpha T_{ij}^\alpha$, where

$$\begin{aligned} T_{ij}^\alpha &= -Jb_i^\dagger b_j \delta(n_i - n_j - \alpha + 1) \\ &= -J \sum_n g_\alpha^n |n+1\rangle_i |n-\alpha\rangle_j \langle n|_i \langle n-\alpha+1|_j \end{aligned} \quad (5)$$

where $g_\alpha^n = \sqrt{(n+1)(n-\alpha+1)}$. Here T_{ij}^α connects states with energy difference ϵ_{ij}^α . A mathematical way of represent-

ing this information is the identity

$$[H_0, T_{ij}^\alpha] = \epsilon_{ij}^\alpha T_{ij}^\alpha, \quad (6)$$

which will be useful later in deriving the canonical transformation operator.

For weak disorder ($V \ll U$), it is evident that T_{ij}^0 represents a low energy hopping process, while T_{ij}^α for $\alpha \neq 0$ changes energy of the state by an amount $\sim \alpha U$ and has to be eliminated by the canonical transform. This breakup of the kinetic energy term follows the method of Girvin *et al* [21] for fermionic Hubbard model with one crucial difference: in the Fermi Hubbard model, the local Hilbert space is constrained by Pauli exclusion and hence $\alpha = 0, \pm 1$, whereas in the Bosonic model, the infinite Hilbert space leads to α taking all possible integer values. In practice, the local Hilbert space is cutoff at some high value of occupancy number, and α will be restricted accordingly. This formalism can be generalized to strong disorder potentials with some more complications, which will be discussed in a future work.

The canonical transformation operator $i\mathcal{S}$ has an expansion in J/U , i.e. $i\mathcal{S} = i\mathcal{S}^1 + i\mathcal{S}^2 + \dots$, where $i\mathcal{S}^m \sim (J/U)^m$ and terms upto $i\mathcal{S}^m$ completely removes high energy terms upto order $J(J/U)^{m-1}$. Using the identity, eqn. (6), it can be shown that

$$i\mathcal{S}^1 = \sum_{\langle ij \rangle} \sum_{\alpha \neq 0} \frac{T_{ij}^\alpha}{\epsilon_{ij}^\alpha} \quad (7)$$

removes all high energy terms $\mathcal{O}(J)$, while

$$\begin{aligned} i\mathcal{S}^2 &= \sum_{\langle ij \rangle \langle kl \rangle} \sum_{\alpha \neq 0} \frac{[T_{ij}^\alpha, T_{kl}^0]}{\epsilon_{ij}^\alpha (\epsilon_{ij}^\alpha + v_k - v_l)} \\ &+ \frac{1}{4} \sum_{\langle ij \rangle \langle kl \rangle} \sum_{\alpha \neq \beta \neq 0} \frac{[T_{ij}^\alpha, T_{kl}^{-\beta}]}{(\epsilon_{kl}^{-\beta} + \epsilon_{ij}^\alpha)} \left[\frac{1}{\epsilon_{ij}^\alpha} - \frac{1}{\epsilon_{kl}^{-\beta}} \right] \end{aligned} \quad (8)$$

removes high energy terms upto $\mathcal{O}(J^2/U)$.

The effective Hamiltonian H^* is then given by

$$H^* = H_0 + \sum_{\langle ij \rangle} T_{ij}^0 + \frac{1}{2} \sum_{\langle ij \rangle \langle kl \rangle} \sum_{\alpha \neq 0} \frac{[T_{ij}^\alpha, T_{kl}^{-\alpha}]}{\epsilon_{ij}^\alpha} \quad (9)$$

which, in the clean case of a Bose Hubbard model without disorder, reduces to

$$H^*(V=0) = H_0 + \sum_{\langle ij \rangle} T_{ij}^0 + \frac{1}{2} \sum_{\langle ij \rangle \langle kl \rangle} \sum_{\alpha \neq 0} \frac{[T_{ij}^\alpha, T_{kl}^{-\alpha}]}{\alpha U} \quad (10)$$

The effective low energy Hamiltonian thus consists of three terms : (a) H_0 which gives the local interaction and disorder potential, (b) T_0 , which represents the low energy hopping, and (c) the last commutator, which can be easily interpreted as a second order perturbation, and takes care of virtual transitions to high energy states.

We would like to note that our canonical transformation improves upon previous formulation by Trefzger *et. al* [22, 23]

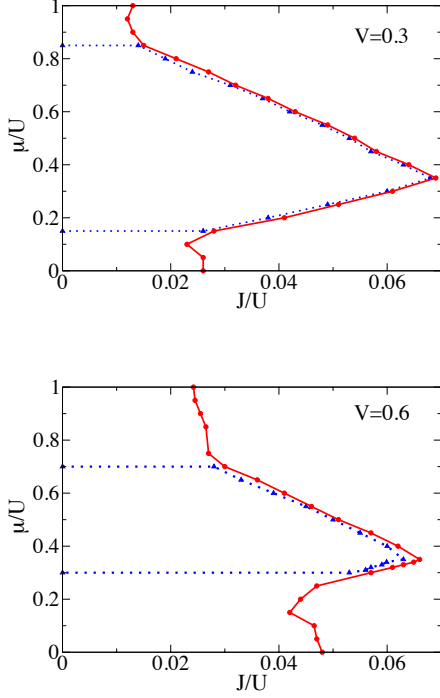


FIG. 1: The zero temperature equilibrium phase diagram of the disordered Bose Hubbard model in the μ/U - J/U plane for (a) $V/U = 0.3$ and (b) $V/U = 0.6$ respectively. The phase to the right of the thick red line is the superfluid phase, while the Mott phase is enclosed by the dotted blue line. The phase in between is the Bose glass phase.

in the following ways: i) It can handle non-uniform states with arbitrary one-body potentials in the local part of the Hamiltonian, which is crucial in treating disordered bosons and ii) It takes into account the full Hilbert space for bosons and is not an expansion around a state with a fixed number of particles on each site. This is crucial to look at the Bose glass phase (and to study properties of bosons in a trap), where the density varies from site to site. This formulation can also handle

more accurately the superfluid phase near the Mott lobes, as it treats all the states in the local Hilbert space on equal footing. In fact, in the clean case, if one keeps only three states in the local Hilbert space (the commensurate density in the Mott state, n_0 and $n_0 \pm 1$), then α is restricted to $0, \pm 1$, and our formulation reduces to that in Ref. 22.

IV. EQUILIBRIUM PHASE DIAGRAM

Starting from the early prediction of Fisher *et. al* [1], the equilibrium phase diagram of disordered Bose Hubbard model has been worked out by several previous authors using various techniques ranging from mean field theory [14] to quantum Monte Carlo techniques [18, 19]. Although our main motivation is to study dynamics of the system when interaction parameters are tuned, we present the equilibrium phase diagram obtained by our method for the sake of completeness. This will also set the stage for our study of dynamics in two ways: (i) the equilibrium ground state forms the initial condition for the dynamics of the system and (ii) we would like to know the trajectory of the system, i.e. whether it goes into the Mott or the Bose glass phase as we ramp up the interaction parameter starting from the superfluid phase.

The ground state is obtained by minimizing the energy in the variational state, which is equivalent to minimizing the expectation of H^* in the mean field state $|\psi_0\rangle$. A straightforward algebra shows that the ground state energy is a sum of six different contributions, $\mathcal{E} = \sum_{r=0}^5 \mathcal{E}_r$, where

$$\mathcal{E}_0 = \sum_{ni} \left[\frac{U}{2} n(n-1) - \mu_i n \right] |f_{ni}|^2 \quad (11)$$

is the local energy corresponding to the interaction and disorder potential,

$$\mathcal{E}_1 = -J \sum_{n\langle ij \rangle} (n+1) f_{n+1i}^* f_{ni} f_{nj}^* f_{n+1j} \quad (12)$$

is the low energy nearest neighbor hopping,

$$\mathcal{E}_2 = \frac{J^2}{2} \sum_{\langle ij \rangle} \sum_{n\alpha \neq 0} (n+1) |f_{ni}|^2 \frac{(n+\alpha+1) |f_{n+\alpha+1j}|^2 - (n-\alpha+1) |f_{n-\alpha+1j}|^2}{\epsilon_{ij}^\alpha} \quad (13)$$

is the second order density-density interaction energy,

$$\mathcal{E}_3 = \frac{J^2}{2} \sum_{\langle ij \rangle} \sum_n (n+1)(n+2) f_{n+2i}^* f_{nj} f_{nj}^* f_{n+2j} \left[\frac{1}{\epsilon_{ij}^1} - \frac{1}{\epsilon_{ij}^{-1}} \right] \quad (14)$$

is a second order pair hopping term where two bosons hop to the nearest neighbor.

$$\mathcal{E}_4 = \frac{J^2}{2} \sum_{\langle ij \rangle \langle ik \rangle} \sum_{n\alpha \neq 0} \frac{f_{n+2i}^* f_{ni}}{\epsilon_{ij}^\alpha} [g_{-\alpha}^n g_\alpha^{n+1} f_{n+\alpha k}^* f_{n+\alpha+1k} f_{n-\alpha+1j}^* f_{n-\alpha+2j} - (\alpha \rightarrow -\alpha)] + h.c. \quad (15)$$

which represents a second order process where two bosons from two different neighboring sites hop onto a site and its reverse process, and finally

$$\mathcal{E}_5 = \frac{J^2}{2} \sum_{\langle ij \rangle \langle jk \rangle} \sum_{n\alpha \neq 0} \frac{|f_{nj}|^2}{\varepsilon_{ij}^\alpha} [g_{-\alpha}^n g_\alpha^{n+\alpha} f_{n+\alpha k}^* f_{n+\alpha+1k} f_{n+\alpha+1i}^* f_{n+\alpha i} - (\alpha \rightarrow -\alpha)] + h.c. \quad (16)$$

which represents a second order next nearest neighbor hopping process.

The energy is then minimized with respect to the variational parameters f_{ni} to obtain the ground state wavefunction. The three different phases are then identified according to the following criterion: The superfluid phase is characterized by a non vanishing superfluid stiffness, which controls the energy of the system for long wavelength distortion of the phase of the Bose Einstein condensate. This can alternatively be thought as the diamagnetic response of the system to a vector potential. In presence of a static vector potential A along the x direction, the hopping parameters acquire an Ahronov-Bohm phase, $J_{ij} \rightarrow J_{ij} e^{A(x_i - x_j)}$, and correspondingly $H \rightarrow H_A$ and $\mathcal{S} \rightarrow \mathcal{S}_A$. The superfluid stiffness can then be calculated as

$$\rho_s = \frac{1}{N_c} \sum_{\mathcal{C}} \frac{\partial^2 \langle H_A^* \rangle_0}{\partial A^2} \Big|_{A=0} \quad (17)$$

where \mathcal{C} denotes disorder configurations and N_c is the number of configurations kept in the disorder average (typically ~ 100 in our calculations). We note that in case of finite disorder potential we will always work with disorder averaged quantities in this paper. Any state with $\rho_s \neq 0$ will be identified as a superfluid phase. In the non-superfluid phase, we distinguish between the Bose glass phase and the Mott insulating phase by the fact that the Bose glass phase has a finite compressibility, while the Mott insulating phase is incompressible. Within our formalism, this implies that $f_{n_0 i} = 1$ for all the lattice sites in all the disorder configurations in commensurate Mott insulator of filling n_0 , while in the Bose glass phase, $\max(f_{n_0 i}) < 1$. We note here that although $f_{n_0 i} = 1$ for all lattice sites in a Mott phase, the canonical transform mixes in virtual number fluctuations in the ground state wavefunction.

In Fig. 1 (a) and (b), we study the phase diagram of the system in the $J/U - \mu/U$ plane, focusing in and around the $n_0 = 1$ Mott plateau, for different disorder strengths $V/U = 0.3$ and $V/U = 0.6$ respectively. The parameter regime to the right of the thick red line represents the superfluid phase with a non-zero superfluid stiffness ($\rho_s \neq 0$). The region enclosed to the left of the blue dotted line is the incompressible Mott phase, while the region in between these two lines represents the Bose glass phase with non zero compressibility but zero superfluid stiffness.

The phase diagram qualitatively captures the basic physics of the disordered Hubbard model. In the atomic limit, ($J = 0$), the system remains in the Mott phase as long as $V/2 < \mu < U - V/2$. The local Hamiltonian H_0 is then optimized by the configuration of one particle on each site. On the other hand, for $\mu < V/2$, there are sites where the local Hamiltonian is optimized by a hole, while for $\mu > U - V/2$, there are

sites where the local Hamiltonian is optimized by double occupancy. Thus the state in this limit has number fluctuations (and hence is compressible) while the local nature of the fluctuations imply that superfluid stiffness is 0. This state is thus in the Bose glass phase. As J/U is increased, the Mott phase first gives rise to a narrow region of Bose glass phase, which then gives way to the superfluid phase. In the region, where the atomic limit ground state is a Bose glass, we see a direct transition between a Bose glass and a superfluid phase.

With increasing disorder strength, we find two distinct features of the phase diagram: (a) The Mott region shrinks with increasing V/U and (b) The direct Bose glass to superfluid transition takes place at larger values of J/U . The first one can be easily explained by noting that with increasing V/U , the width of the Mott phase in the atomic limit ($U - V/2 > \mu > V/2$) decreases. The second feature is explained by the fact that stronger disorder leads to stronger scattering and hence larger values of J/U is required to restore phase coherence and hence superfluidity in the system.

Before concluding this section, we note that analogous phase diagrams, which are in qualitative agreement with ours, have been derived using single-site and multi-site mean-field theories [14–16], strong-coupling expansions [17] and quantum Monte Carlo [18–20]. All of these methods concur with ours regarding the qualitative features of the phase diagram such as presence of a glassy region between the superfluid and Mott phase in the presence of disorder and the increase in the extent of this glassy region towards the edge of the Mott lobes.

V. DYNAMICS IN THE DISORDERED BOSE HUBBARD MODEL

Our main goal in this paper is to study the dynamics of the disordered Bose Hubbard model when a Hamiltonian parameter (in our case the hopping J) is changed in time. Although a lot of work has been done on the equilibrium phase diagram of the disordered Bose Hubbard model, very little is known about the dynamics of this system. In this context it is worth noting that the variational wavefunction and the canonical transformation is especially well suited to treat the dynamics in this system. For a dynamically changing system one can write down a variational wavefunction of the form

$$|\psi(t)\rangle = e^{-iS[J(t)]} |\psi_0(t)\rangle \quad |\psi_0(t)\rangle = \prod_i \sum_n f_{ni}(t) |n\rangle_i \quad (18)$$

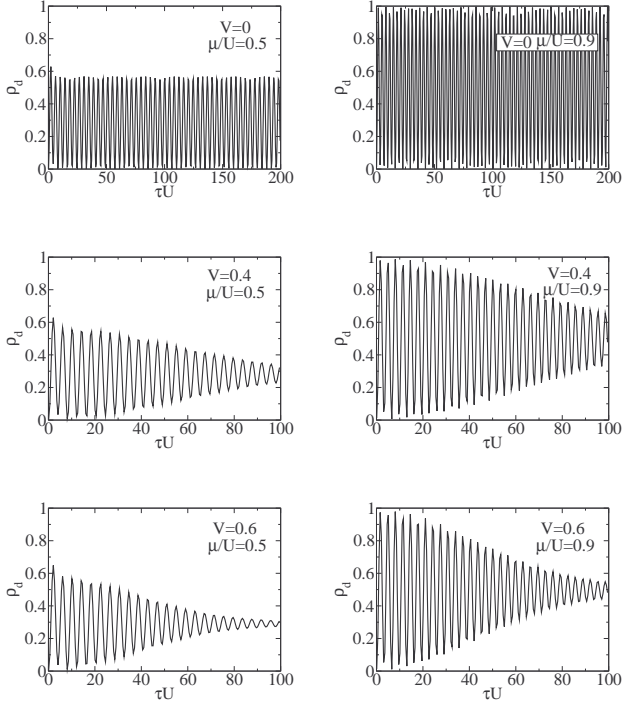


FIG. 2: Disordered averaged defect density as a function of rate of change of hopping for: (a) top panel: clean case with $\mu/U = 0.5$ (left) and $\mu/U = 0.9$ (right) (b) middle panel: disorder potential $V/U = 0.4$ with $\mu/U = 0.5$ (left) and $\mu/U = 0.9$ (right) (c) lower panel: disorder potential $V/U = 0.6$ with $\mu/U = 0.5$ (left) and $\mu/U = 0.9$ (right).

where the canonical transformation is evaluated with the instantaneous value of the parameter $J(t)$. Note that since our canonical transform was based on the idea of eliminating terms in the Hamiltonian, which connects states differing by a large energy $\sim U$, this would lead to a coarse grained dynamics valid for timescales much larger than U^{-1} . Further, since the canonical transform was not an expansion around a particular state (like the Mott state), this can faithfully capture the evolution of the excitations that are inevitably created during time evolution.

The Schrodinger equation can then be written as

$$i|\dot{\psi}_0\rangle = (H^* - \dot{S}^*)|\psi_0\rangle \quad (19)$$

where $\dot{S}^* = e^{iS}\dot{S}e^{-iS}$ and the initial ground state is evolved according to this equation.

At this point it is useful to look at the particular form of dynamics we are interested in. We start our system in the ground state with an initial value of J_i , which puts it in the superfluid phase. We then decrease J linearly to a very small value J_f close to the atomic limit with a rate τ^{-1} . We then ramp back to our initial value J_i with the same ramp rate. The

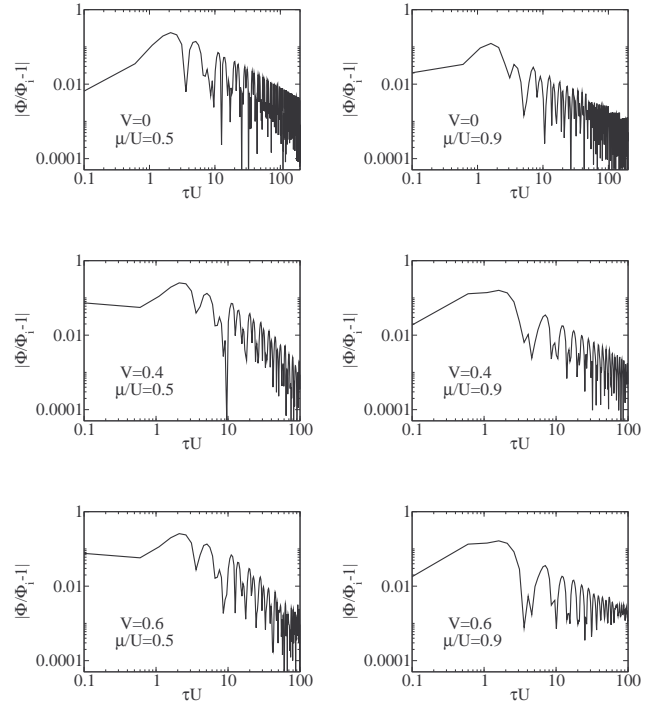


FIG. 3: Relaxation of superfluid order parameter as a function of rate of change of hopping. The deviation of $|\Phi(2\tau)/\Phi(0)|$ from 1 is plotted for: (a) top panel: clean case with $\mu/U = 0.5$ (left) and $\mu/U = 0.9$ (right) (b) middle panel: disorder potential $V/U = 0.4$ with $\mu/U = 0.5$ (left) and $\mu/U = 0.9$ (right) (c) lower panel: disorder potential $V/U = 0.6$ with $\mu/U = 0.5$ (left) and $\mu/U = 0.9$ (right).

explicit time dependence of the hopping parameter is given by

$$\begin{aligned} J(t) &= J_i + (J_f - J_i)\frac{t}{\tau} \quad t < \tau \\ &= J_f + (J_i - J_f)\frac{t}{\tau} \quad t > \tau \end{aligned} \quad (20)$$

The effective Hamiltonian H^* gives rise to energy scales of J , U and J^2/U , while the \dot{S} term generates scales of $\Delta J/(U\tau)$, $\Delta J J(t)/U^2\tau^2$ etc. We assume $U\tau > 1$ (later we will mostly be interested in the regime $U\tau \gg 1$), and we will only keep the first order term \dot{S}^1 in the dynamical equations. This leads to a notable simplification; since $i\dot{S}^1 \propto iS^1$, $i\dot{S}^* = i\dot{S}$, i.e. there is no Berry phase contribution from rotating the $i\dot{S}$ term. We note that this simplification goes away if we include higher order terms in iS .

We are interested in the excitations created as we ramp down to the atomic limit and ramp back up to the initial value of J/U . To study this we look at the defect density which, for a given disorder configuration is given by

$$\rho_d(\tau) = \frac{1}{N_s} \sum_i 1 - |\langle \psi_0^i(2\tau) | \psi_0^i(0) \rangle|^2 \quad (21)$$

where $|\psi_0^i(t)\rangle = \sum_n f_{ni}(t)|n\rangle_i$ is the local Gutzwiller wave-

function at time t . Note that since the final and initial values of J/U are same, the canonical transformation operator does not affect this definition of defect density. For the disordered Bose Hubbard model we study the defect density averaged over many disorder realizations. The defect density is plotted as a function of the time constant τ for various values of V/U and μ/U in Fig 2. The top panel shows the clean case ($V = 0$) results for (left): $\mu/U = 0.5$, where one passes close to the Mott lobe tip as one decreases the hopping J , and (right): $\mu/U = 0.9$, which is far away from the Mott tip. The defect density shows oscillatory behaviour with τ with the large τ ($U\tau \gg 1$) limit exhibiting an envelope which is constant with τ . We note that we have taken care to fix the gauge during the time evolution and hence the oscillations are not a result of the system sampling different gauge configurations in time. Rather, the return of the system to its initial state ($\rho_d = 0$) for certain rates of change of hopping has similar origins as found in Ref. 24, where the system was found to return to its initial state under the influence of a periodic drive for certain drive frequencies. The constant envelope characterizes the fact that within the canonical transformation there is a low energy state orthogonal to the initial ground state (with the degeneracy broken on a scale of $\sim J^2/U$). The limiting constant value is ~ 1 away from the Mott tip, where it is easy to create excitations and goes to ~ 0.6 near the Mott tip. The middle panel shows the defect density as a function of the ramp rate for a disordered system characterized by $V/U = 0.4$, while the lower panel shows a system with $V/U = 0.6$. The oscillatory behaviour persists, but presence of disorder damps the oscillations, with the defect density showing an exponential decay with the inverse ramp rate. Disorder leads to scattering and lifts the degeneracy of the low lying state, thus leading to an exponential decay of the defect density. It is also clear by comparing the middle and the lower panel figures that as V/U increases, the damping timescale becomes smaller. In the large τ limit, the defect density goes to a constant value, which is almost independent of V/U and depends crucially on μ/U . For $\mu/U = 0.5$, this value is ~ 0.3 , while for $\mu/U = 0.9$, this value increases to ~ 0.6 . The finite value of the defect density in the large τ limit is expected, as the system starts from superfluid phase with associated gapless modes and hence there is no excitation gap to protect defect creation in the slow ramping limit.

We have also studied the evolution of the superfluid order parameter

$$\Phi(t) = \frac{1}{N_s} \sum_i \langle \psi(t) | b_i | \psi(t) \rangle \quad (22)$$

as the hopping is ramped down and up. To ensure normalization it is easiest to look at the ratio $r = \Phi(2\tau)/\Phi(0)$ and then construct the disorder average of this quantity. The disorder averaged r goes to 1 in the large τ limit and hence we look at $|r| - 1$ to determine how the order parameter relaxes to its initial value as a function of the ramp rate. This quantity is plotted in Fig. 3 for the clean case (top panel) and the disordered case for $V/U = 0.4$ (middle panel) and $V/U = 0.6$ (lower panel). In the clean case, the quantity $|r| - 1$ clearly

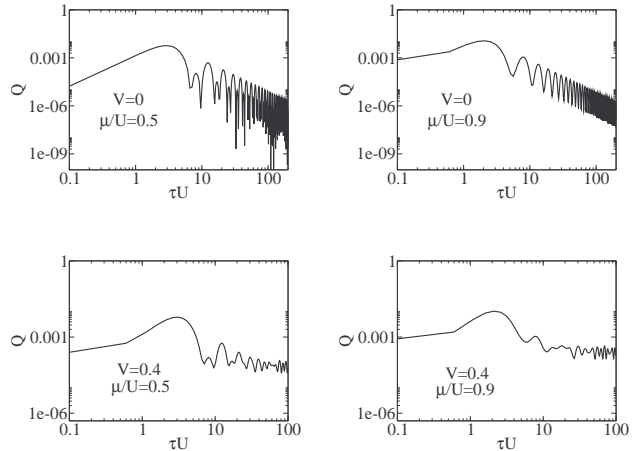


FIG. 4: Residual energy in the system as a function of rate of change of hopping for: (a) top panel: clean case with $\mu/U = 0.5$ (left) and $\mu/U = 0.9$ (right) (b) bottom panel: disordered potential $V/U = 0.4$ with $\mu/U = 0.5$ (left) and $\mu/U = 0.9$ (right).

shows a power-law scaling with an asymptotic $1/\tau$ envelope on top of oscillations in the large τ limit. The relaxation in the disordered case is not so simple. Although $|r| - 1$ goes down with τ , we have not been able to clearly extract either a power law or an exponential scaling from the large τ limit. There is a substantial window of τ values, where a $1/\tau$ power law can be defined, but the data seems to deviate from this scaling for larger values of τ .

We also study the residual energy pumped into the system in the process of ramping down the hopping and returning back to the original value. This is important as there is a lack of in-situ measurements of temperature in optical lattices and the energy pumped into the system is often taken as a bound on the amount of heating in the system. The excess energy of the system in the final state is given by

$$Q = \langle \psi(2\tau) | H | \psi(2\tau) \rangle - \langle \psi(0) | H | \psi(0) \rangle \quad (23)$$

The excess energy of the system as a function of ramp rate is shown in Fig. 4. In the clean case, the energy decays with τ , with a $1/\tau^2$ envelope in the large τ limit. One way to understand this is that within a Gross-Pitaevsky description, the lowest order dependence of the energy on the order parameter is $E \sim |\Phi|^2$, and so, a $1/\tau$ relaxation of the order parameter leads to a $1/\tau^2$ energy relaxation in the system. In the disordered case, although the excess energy decreases with τ , numerical accuracy of the data forbids a clear extraction of an asymptotic limit.

VI. CONCLUSIONS

In this paper, we have studied the equilibrium and non-equilibrium properties of the disordered Bose Hubbard model using a new variational wavefunction approach. Our variational wavefunction implements the canonical Schrieffer-

Wolf transformation, which has been extensively used for strongly interacting Fermions to the case of strongly repulsive Bosons in a non-uniform potential background. We have determined the equilibrium phase diagram of the system, which shows the expected Mott insulator, Bose glass and the superfluid phases. Our phase diagram is qualitatively similar to the phase diagram obtained by more sophisticated techniques.

We have also studied the non-equilibrium properties of the disordered bosons within this variational approach. We have focused on the specific dynamic process, where, starting from the system in its ground state in the superfluid phase, the hopping parameter J is ramped down linearly with a rate τ^{-1} to a value very close to 0. The hopping is then ramped back with the same rate to its initial value. We look at the response of the system to this non-equilibrium cyclic process by studying the density of excitations, the superfluid order parameter and the energy of the excitations in the final state obtained from the time evolution of the initial ground state. In the clean system ($V = 0$), we find that all the three quantities show oscillatory behaviour as a function of the inverse ramp rate τ . The asymptotic envelope of the defect density is a constant, while the order parameter and the energy decays as $1/\tau$ and $1/\tau^2$ respectively in the large τ ($U\tau \gg 1$) limit. In the disordered system, the oscillations persist, although they are damped by disorder scattering. The defect density, as a function of the inverse ramp rate, oscillates with an exponentially decaying envelope. The decay of the defect density as a function of τ increases with increasing V/U , while the value of the excitation density in the large $\tau \rightarrow \infty$ limit is independent of

V/U , but depends on the value of μ/U , i.e. it increases as one moves away from the tip of the Mott lobe. The deviation of the superfluid order parameter from its initial value as well as the energy pumped into the system decays with decreasing ramp rate, but numerical noise prohibits a clear extraction of a large τ asymptotic scaling.

The variational wavefunction and the associated canonical transform used in this paper provides a new analytic way of treating the problem of disordered strongly interacting bosons on a lattice. In fact, this technique can be used to study any one body potential (including harmonic trap potentials relevant to the cold atom experiments). In its current form, the variational wavefunctions capture the essential physics of the superfluid, Bose glass and Mott insulator phases in the low disorder limit $V/U \ll 1$. Although we have stretched the technique to $V/U \sim 0.6$, the numerical accuracy of the method decreases and quantitative match of the phase diagram with the Monte Carlo results deteriorates. A more complete formulation, which is beyond the scope of this paper, would incorporate the fact that for $U > |v_i - v_j| \gg J$, the hopping on the bond between i and j is completely frozen, while for $v_i - v_j \sim nU$, there is a low energy hopping process which changes the number of multiple occupancies in the system. Further development along these lines would lead to higher numerical accuracy and wider applicability of this new technique.

This work is supported by AFOSR JQI-MURI, ARO-DARPA-OLE, and NSF-JQI-PFC.

-
- [1] M. P. A. Fisher, P. B. Weichman, G. Grinstein, and D. S. Fisher, *Phys. Rev. B* **40**, 546 (1989), URL <http://link.aps.org/doi/10.1103/PhysRevB.40.546>.
- [2] P. A. Crowell, F. W. Van Keuls, and J. D. Reppy, *Phys. Rev. B* **55**, 12620 (1997), URL <http://link.aps.org/doi/10.1103/PhysRevB.55.12620>.
- [3] G. A. Csáthy, J. D. Reppy, and M. H. W. Chan, *Phys. Rev. Lett.* **91**, 235301 (2003), URL <http://link.aps.org/doi/10.1103/PhysRevLett.91.235301>.
- [4] Y. Liu, K. A. McGreer, B. Nease, D. B. Haviland, G. Martinez, J. W. Halley, and A. M. Goldman, *Phys. Rev. Lett.* **67**, 2068 (1991), URL <http://link.aps.org/doi/10.1103/PhysRevLett.67.2068>.
- [5] H. S. J. van der Zant, W. J. Elion, L. J. Geerligs, and J. E. Mooij, *Phys. Rev. B* **54**, 10081 (1996), URL <http://link.aps.org/doi/10.1103/PhysRevB.54.10081>.
- [6] R. Yu, C. F. Miclea, F. Weickert, R. Movshovich, A. Paduan-Filho, V. S. Zapf, and T. Roscilde (2012), arXiv:1204.5409.
- [7] G. Roati, C. D'Errico, L. Fallani, C. Fattori, M. and Fort, M. Zaccanti, G. Modugno, M. Modugno, and M. Inguscio, *Nature* **453**, 895 (2008), URL <http://dx.doi.org/10.1038/nature07071>.
- [8] M. White, M. Pasienski, D. McKay, S. Q. Zhou, D. Ceperley, and B. DeMarco, *Phys. Rev. Lett.* **102**, 055301 (2009), URL <http://link.aps.org/doi/10.1103/PhysRevLett.102.055301>.
- [9] M. Robert-de Saint-Vincent, J.-P. Brantut, B. Allard, T. Plisson, L. Pezzé, L. Sanchez-Palencia, A. Aspect, T. Bourdel, and P. Bouyer, *Phys. Rev. Lett.* **104**, 220602 (2010), URL <http://link.aps.org/doi/10.1103/PhysRevLett.104.220602>.
- [10] I. Bloch, J. Dalibard, and W. Zwerger, *Rev. Mod. Phys.* **80**, 885 (2008), URL <http://link.aps.org/doi/10.1103/RevModPhys.80.885>.
- [11] J. Biddle, B. Wang, D. J. Priour, and S. Das Sarma, *Phys. Rev. A* **80**, 021603 (2009), URL <http://link.aps.org/doi/10.1103/PhysRevA.80.021603>.
- [12] T. Kinoshita, T. Wenger, and D. S. Weiss, *Nature* **440**, 900 (2006), URL <http://dx.doi.org/10.1038/nature04693>.
- [13] N. Strohmaier, D. Greif, R. Jördens, L. Tarruell, H. Moritz, T. Esslinger, R. Sensarma, D. Pekker, E. Altman, and E. Demler, *Phys. Rev. Lett.* **104**, 080401 (2010), URL <http://link.aps.org/doi/10.1103/PhysRevLett.104.080401>.
- [14] P. Buonsante, V. Penna, A. Vezzani, and P. B. Blakie, *Phys. Rev. A* **76**, 011602 (2007), URL <http://link.aps.org/doi/10.1103/PhysRevA.76.011602>.
- [15] K. V. Krutitsky, A. Pelster, and R. Graham, *New Journ. Phys.* **8**, 187 (2006), URL [doi:10.1088/1367-2630/8/9/187](http://dx.doi.org/10.1088/1367-2630/8/9/187).
- [16] P. Pisarski, R. M. Jones, and R. J. Gooding, *Phys. Rev. A* **83**, 053608 (2011), URL <http://link.aps.org/doi/10.1103/PhysRevA.83.053608>.
- [17] J. K. Freericks and H. Monien, *Phys. Rev. B* **53**, 2691 (1996), URL <http://link.aps.org/doi/10.1103/PhysRevB.53.2691>.

- [18] L. Pollet, N. V. Prokof'ev, B. V. Svistunov, and M. Troyer, Phys. Rev. Lett. **103**, 140402 (2009), URL <http://link.aps.org/doi/10.1103/PhysRevLett.103.140402>.
- [19] V. Gurarie, L. Pollet, N. V. Prokof'ev, B. V. Svistunov, and M. Troyer, Phys. Rev. B **80**, 214519 (2009), URL <http://link.aps.org/doi/10.1103/PhysRevB.80.214519>.
- [20] F. Lin, E. S. Sørensen, and D. M. Ceperley, Phys. Rev. B **84**, 094507 (2011), URL <http://link.aps.org/doi/10.1103/PhysRevB.84.094507>.
- [21] A. H. MacDonald, S. M. Girvin, and D. Yoshioka, Phys. Rev. B **37**, 9753 (1988), URL <http://link.aps.org/doi/10.1103/PhysRevB.37.9753>.
- [22] C. Trefzger and K. Sengupta, Phys. Rev. Lett. **106**, 095702 (2011), URL <http://link.aps.org/doi/10.1103/PhysRevLett.106.095702>.
- [23] A. Dutta, C. Trefzger, and K. Sengupta (2011), arXiv:1111.5085.
- [24] S. Mondal, D. Pekker, and K. Sengupta (2012), arXiv:1204.6331.